ISTITUTO NAZIONALE DI FISICA NUCLEARE

Sezione di Lecce

INFN/AE–98/02
8 Gennaio 1998

V. Elia, E. Gorini, F. Grancagnolo:

CHARMONIUM PRODUCTION AT FNAL/E771

PACS: 13.85.Ni, 13.85.Lg

Published by ***SIS–Pubblicazioni***
Laboratori Nazionali di Frascati

INFN – Istituto Nazionale di Fisica Nucleare
Sezione di Lecce

INFN/AE–98/02
8 Gennaio 1998

CHARMONIUM PRODUCTION AT FNAL/E771

V. Elia, E. Gorini, F. Grancagnolo
Department of Physics and INFN–Sezione di Lecce, Via Arnesano, I–73100 Lecce, Italy

Abstract

We present some results on Charmonium states produced in p-Si interactions at $\sqrt{s} = 38.7\ GeV$. The data samples are constituted by about 12000 J/ψ and 200 ψ' decaying into opposite sign muons. The total cross sections are $B\sigma = (21.8 \pm 0.26 \pm 1.4)\ nb/nucleon$ for J/ψ and $B\sigma = (0.36 \pm 0.04 \pm 0.024)\ nb/nucleon$ for ψ'. The J/ψ and ψ' x_F and p_T distributions are compared to recent results from experiment E789 at the same energy and to leading order QCD predictions using the MRS D0 parametrization for the parton structure function. The measured shapes of the J/ψ and ψ' differential cross sections, except for the $d\sigma/dx_F$ at small x_F, agree very well with the prediction, except for an overall scale factor. We also present the $cos\theta$ differential cross section of the J/ψ which indicates unpolarized production in contrast with color octet models predictions.

1 Introduction

Hadronic production of charmonium states is one of the most studied processes in high energy physics. In spite of this experimental effort, the mechanisms of quarkonium production are not well understood, and calculations of higher order contributions are still missing. In addition, the formation of the $c\bar{c}$ bound states is a non-perturbative QCD process and requires some understanding of the evolution from the quark-antiquark color octet to the physical quarkonium states. The renewed interest in these subjects, owing to Tevatron collider results [3], has led to a better theoretical understanding of these mechanisms with the development of a new model in the past couple of years [1, 2]. One of the

features of this new model is that it predicts high transverse polarization of quarkonium states.

The study of inclusive J/ψ production is complicated by additional contributions from radiative decays of higher-mass states ($\chi_{i=0,1,2}$ and ψ') to the direct production, making comparison with theory more difficult.

2 Experimental setup

2.1 Beam and target

The data were collected at the High Intensity Laboratory in a primary proton beam at Fermilab with the E771 spectrometer during a short run of 5 weeks.

The 800 GeV/c beam, of average intensity 4×10^7 proton/s per 23 s spill every 57 s, interacted with a silicon target consisting of 12 foils, each 2 mm thick and spaced 4 mm apart, for a total of 5.3 % of an interaction length. The resulting average interaction rate was approximately 2 MHz.

The beam was monitored by means an ion chamber and beam silicon strip detectors placed along the beam line, which gave a total integrated number of live protons on target of 1.313×10^{13} with an error of approximately 5 % dominated by the uncertainty in the efficiency of the beam silicon detector.

2.2 Spectrometer

The E771 spectrometer [4, 5] was optimized for the observation of dimuons coming from J/ψ's generated in the decays of heavy quark states. It consisted of a silicon microstrip detector, a tracking section upstream and downstream of an analysis magnet, an electromagnetic calorimeter and a muon detector placed after a hadron absorber. Neither the microstrip detector nor the calorimeter was used for the analysis described here.

The tracking section consisted of 22 planes of MWPC and 9 planes of drift chambers to define the charged particle trajectories upstream of the analysis magnet and of 12 planes of drift and 6 of drift-pad [6] chambers downstream of the magnet. All chambers were deadened in a region around the beam axis with a resulting minimum acceptance angle of 25 mrad. The analysis magnet, a dipole with 185×90 cm^2 aperture, provided a p_T kick of 0.82 GeV/c in the horizontal plane.

The muon detector, located downstream of a 3 m thick hadron absorber, made of steel (copper in the central part), consisted of three planes of resistive plate counters (RPC's) and three planes of scintillators separated by steel, concrete and lead absorbers. The RPC's are thin gap (2 mm) gas devices operating in the streamer mode under a high uniform electric field (40 kV/cm). The charge produced by the streamer process is picked up by external copper pads [7].

The single and dimuon triggers, entirely based on the RPC signals, defined a muon as the triple coincidence among a projective set of pads belonging to the three RPC planes [8, 9]. The minimum momentum required for a muon to penetrate the absorbers and produce a signal in the third RPC plane was 10 GeV/c in the central part and about 6 GeV/c at wider angles.

Further details of the E771 spectrometer can be found elsewhere [5].

3 Data analysis

The collected data amounted to about 130 million dimuon triggers and 60 million single muon triggers recorded on 1200 exabyte cassette tapes. The 130 million dimuon trigger events were processed with a fast filter program which, starting from muon candidates, defined as the coincidence of at least 4 out of the 3 RPC and 3 scintillator planes, reconstructed only the muon tracks downstream of the analysis magnet. In the subsequent analysis, these muons were fully tracked in all chambers and through the analysis magnet. Opposite sign dimuons, constrained to a common vertex, were selected. Only the pair with the best vertex constrained fit χ^2 was considered for this analysis.

The overall reconstruction efficiencies and acceptances were obtained by generating about 10^6 Monte Carlo (MC) events for the J/ψ and 10^5 for the ψ'. The first iteration differential distributions used in the MC were taken from earlier experiments at lower energy. The mesons were assumed to decay isotropically. The decay muons were propagated through a GEANT simulation of the E771 detector taking into account the measured chamber and trigger efficiencies [7, 8, 9] and the contribution of multiple scattering. To simulate realistic noise in the detector, the generated events were superimposed on real events. In the high-end x_F bins the distribution of reconstructed masses was fit with two Gaussians while the mass distribution on the midrange bins was fit with three Gaussians. In the latter case the widest Gaussian was considered as background because an independent study showed that events in the wider Gaussian were primarily cases in which the reconstructed x_F was more than 3σ different than the generated one. The ranges of x_F and p_T over which the experiment is sensitive are respectively, $-0.05 < x_F < 0.25$ and $p_T < 3.5\ GeV/c$. The average relative resolutions are 6.0 % in x_F and 6.7 % in p_T. The range for the angular distribution is $-0.8 < cos\theta < 0.8$.

4 Experimental results

4.1 Total cross sections

Fig. 1 shows the invariant mass spectrum of the selected opposite sign dimuons. A total of 11660±139 J/ψ and 218±24 ψ' are obtained from fits to the background subtracted number of events in the two peaks. The dashed line represents the background, fitted to the function:

$$\frac{a}{m_{\mu\mu}^3} exp(-bm_{\mu\mu}), \tag{1}$$

which is mainly due to muons from π and K decays, to the Drell-Yan process and to charm production. Contributions from B mesons are negligible.

The total inclusive cross section per nucleon has been evaluated assuming an atomic weight dependence A^α, with $\alpha = 0.920 \pm 0.008$ [10]. The choice of this value is justified by the adequate description of the available data [10] for a silicon target ($A = 28$) and, because in our range of x_F and p_T, α appears to be fairly constant [10, 11].

The inclusive J/ψ production cross section is:

$$B(J/\psi \to \mu^+\mu^-)\sigma(J/\psi) = (21.8 \pm 0.3_{stat} \pm 1.4_{syst})\ nb/nucleon\,.$$

The systematic error is dominated by the uncertainty in the total efficiency (5 %) and luminosity (5 %). This measurement is in good agreement with Ref. [12] where the total inclusive cross section is calculated at leading order, taking into account relativistic corrections and assuming an empirical $K = 1.7$ factor for high order corrections.

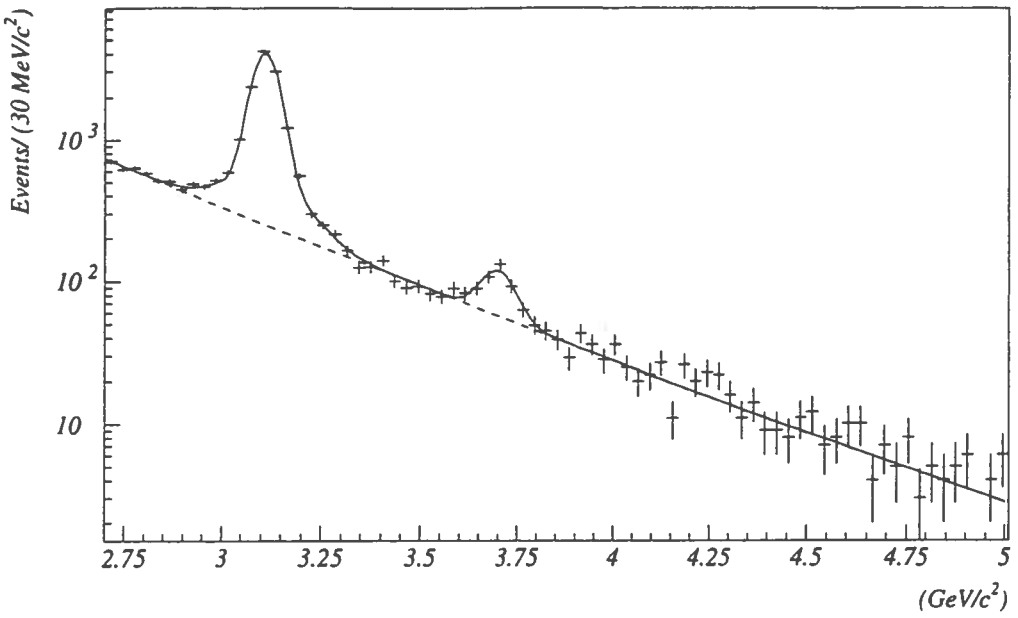

FIG. 1– *Invariant mass spectrum of the $\mu^+\mu^-$ pairs. The dashed line is the continuum background as described in the text.*

Applying a similar technique to the ψ' we determined the inclusive ψ' production cross section to be:

$$B(\psi' \to \mu^+\mu^-)\sigma(\psi') = (0.360 \pm 0.040_{stat} \pm 0.024_{syst})\ nb/nucleon\,.$$

We have compared our J/ψ $B\sigma$ result to previous experiments (correcting them for the latest branching ratio measurement and atomic dependence) and to another experiment [13] at the same energy. The data [14] in Fig. 2 have been fit to a threshold production parametrization as a function of $\sqrt{s}$

$$B(J/\psi \to \mu^+\mu^-)\sigma(J/\psi) = \sigma_0(1 - M_{J/\psi}/\sqrt{s})^\beta$$

obtaining $\sigma_0 = (60 \pm 6)$ nb/nucleon and $\beta = 11.8 \pm 0.5$.

From our measured total inclusive cross sections we also obtain the ratio

$$\frac{B(\psi' \to \mu^+\mu^-)\sigma(\psi')}{B(J/\psi \to \mu^+\mu^-)\sigma(J/\psi)} = (1.65 \pm 0.20)\%$$

shown in Fig. 3 together with the values obtained by other experiments as a function of $\sqrt{s}$.

From theoretical predictions about the contribution of χ_{c1}, χ_{c2} and ψ' to J/ψ production [12] (using MRS D0' structure functions [15] with $\mu = M/2$ where M is the mass of the resonance) one can extract the direct J/ψ cross section. Using the branching ratios taken from Ref. [16], the ratio

$$\frac{\sigma(\psi')}{\sigma_{dir}(J/\psi)} = 0.26 \pm 0.06$$

obtained is compatible with 0.24 ± 0.03 as expected in the framework of the colour evaporation model [17].

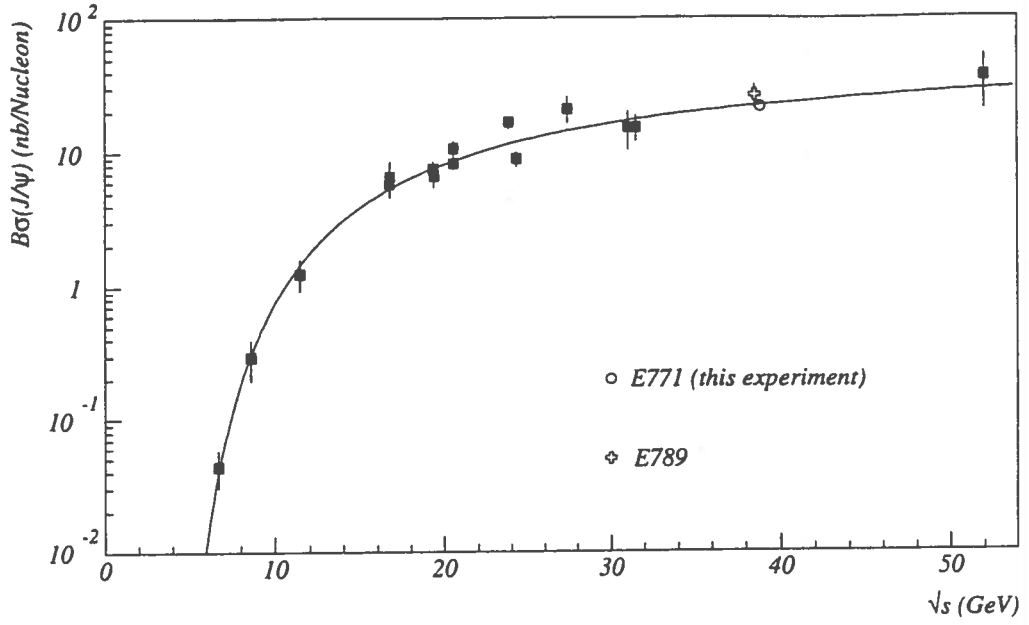

FIG. 2– *J/ψ cross section as a function of the center of mass energy measured by different experiments. Superimposed to the data is the fit described in the text.*

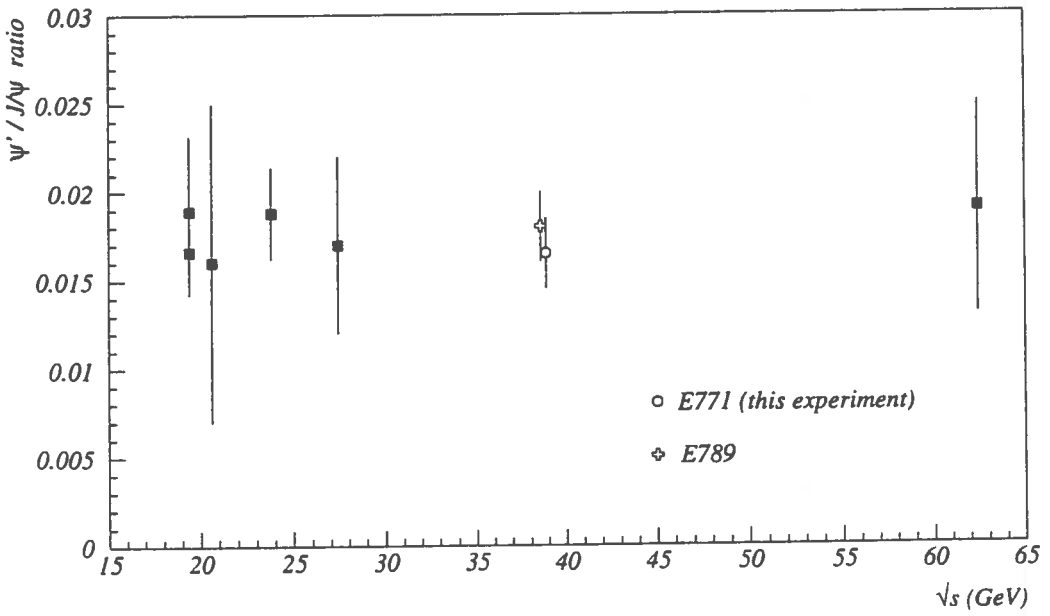

FIG. 3– *The $B\sigma(\psi')/B\sigma(J/\psi)$ ratio versus the center of mass energy.*

4.2 Differential cross sections

The differential distributions have been extracted by fitting the mass spectra in each of the x_F and p_T bins with the resolution functions of the two resonances (the sum of two Gaussians for the J/ψ and a single Gaussian for the ψ') over the described background. The use of two Gaussians for the J/ψ, suggested by Monte Carlo studies, is motivated by the different quality of the information obtainable in highly populated hit regions. The mass resolution of the spectrometer depends on x_F, ranging from 20 MeV/c^2 at $x_F = -0.05$ to about 100 MeV/c^2 at $x_F = 0.25$, while it is totally independent of the transverse momentum, in agreement with Monte Carlo simulation.

In order to minimize systematics, the procedure for extracting the differential distributions was iterated by inserting into the Monte Carlo the extracted x_F and p_T distributions, corrected for the resulting acceptances and efficiencies, until convergence and stability of the result was reached.

The values of the branching ratios $B(J/\psi \to \mu^+\mu^-)$ and $B(\psi' \to \mu^+\mu^-)$ have been taken from Ref. [16].

The measured differential cross sections for each of the x_F and p_T bins are listed in Tab. 1 for the J/ψ and in Tab. 2 for the ψ'. In addition to the errors shown, there are overall systematic uncertainties of 8 % for the J/ψ and 23 % for the ψ'. These systematic errors are mainly due to the uncertainties in luminosity, branching ratios and acceptance.

TAB. 1– *J/ψ cross section for each bin of x_F and p_T. There is an overall systematic error of* 8 %.

x_F bin	$d\sigma/dx_F$	p_T bin	$d\sigma/dp_T^2$
	$[nb/nucleon]$	$[GeV/c]$	$[nb(GeV/c)^{-2}/nucleon]$
$-0.05 \div -0.03$	1309 ± 78	$0.0 \div 0.3$	197 ± 17
$-0.03 \div -0.01$	1352 ± 70	$0.3 \div 0.6$	175.9 ± 9.8
$-0.01 \div 0.01$	1327 ± 56	$0.6 \div 0.9$	134.9 ± 5.9
$0.01 \div 0.03$	1242 ± 48	$0.9 \div 1.2$	101.1 ± 4.2
$0.03 \div 0.05$	1134 ± 44	$1.2 \div 1.5$	64.7 ± 2.8
$0.05 \div 0.07$	963 ± 46	$1.5 \div 1.8$	41.5 ± 2.3
$0.07 \div 0.09$	776 ± 35	$1.8 \div 2.1$	22.6 ± 1.6
$0.09 \div 0.11$	701 ± 36	$2.1 \div 2.4$	12.3 ± 1.4
$0.11 \div 0.13$	591 ± 35	$2.4 \div 2.8$	4.8 ± 0.5
$0.13 \div 0.15$	508 ± 34	$2.8 \div 3.2$	1.84 ± 0.27
$0.15 \div 0.17$	463 ± 39	$3.2 \div 3.6$	0.59 ± 0.20
$0.17 \div 0.19$	427 ± 38		
$0.19 \div 0.21$	353 ± 40		
$0.21 \div 0.23$	254 ± 28		
$0.23 \div 0.25$	294 ± 39		

The $d\sigma/dx_F$ cross sections per nucleon are shown in Fig. 4 as a function of the fractional

TAB. 2– *ψ' cross section for each bin of x_F and p_T. There is an overall systematic error of 23 %.*

x_F bin	$d\sigma/dx_F$ $[nb/nucleon]$	p_T bin $[GeV/c]$	$d\sigma/dp_T^2$ $[nb(GeV/c)^{-2}/nucleon]$
$-0.06 \div -0.02$	148 ± 59	$0.0 \div 0.4$	25.1 ± 8.0
$-0.02 \div 0.02$	199 ± 45	$0.4 \div 0.7$	23.3 ± 5.4
$0.02 \div 0.06$	127 ± 30	$0.7 \div 1.0$	15.3 ± 4.0
$0.06 \div 0.10$	82 ± 25	$1.0 \div 1.4$	13.6 ± 2.2
$0.10 \div 0.14$	87 ± 18	$1.4 \div 2.4$	2.4 ± 0.7
$0.14 \div 0.18$	54 ± 12	$2.4 \div 3.4$	0.51 ± 0.26
$0.18 \div 0.22$	37 ± 17		
$0.22 \div 0.26$	32 ± 13		

longitudinal momentum x_F of the J/ψ and ψ'. The data have been fit with an empirical function of the form

$$\frac{d\sigma}{dx_F} = A(1- \mid x_F \mid)^n . \tag{2}$$

The fit parameters are shown in Tab. 3. The first row in the table shows the results of a fit to all the data points, while the second row (corresponding to the line fit of Fig. 4) shows the fit excluding the two negative x_F values. The fourth row in Tab. 3 lists the fit parameters for ψ' when n is forced to be equal to the corresponding value of the J/ψ fit.

TAB. 3– *Results of the fits performed on the differential distributions as described in the text.*

meson	function	A	n	χ^2/DOF
J/ψ	$A(1- \mid x_F \mid)^n$	$1424 \pm 31\ nb$	6.54 ± 0.23	1.65
J/ψ	$A(1- \mid x_F \mid)^n$	$1386 \pm 33\ nb$	6.38 ± 0.24	0.92
ψ'	$A(1- \mid x_F \mid)^n$	$178 \pm 29\ nb$	6.7 ± 1.3	0.24
ψ'	$A(1- \mid x_F \mid)^n$	$172 \pm 17\ nb$	$6.38(fixed)$	0.26
J/ψ	$Aexp(-np_T^2)$	$182 \pm 5\ nb(GeV/c)^{-2}$	$0.54 \pm 0.01\ (GeV/c)^{-2}$	0.93
J/ψ	$Aexp(-np_T^2)$	$185 \pm 5\ nb(GeV/c)^{-2}$	$0.55 \pm 0.01\ (GeV/c)^{-2}$	0.60
ψ'	$Aexp(-np_T^2)$	$27 \pm 4\ nb(GeV/c)^{-2}$	$0.61 \pm 0.08\ (GeV/c)^{-2}$	1.02

Analogously, the $d\sigma/dp_T^2$ cross sections per nucleon versus the transverse momentum of the produced meson, for both charmonium states, are shown in Fig. 5. The data were parametrized by:

$$\frac{d\sigma}{dp_T^2} = Aexp(-np_T^2) . \tag{3}$$

Again, the fit parameters are listed in Tab. 3. The fifth row in the table shows the results of a fit to all data points. The fit for the J/ψ has been also performed by excluding the last two points in order to directly compare our result to the one of Fermilab E789 [13]

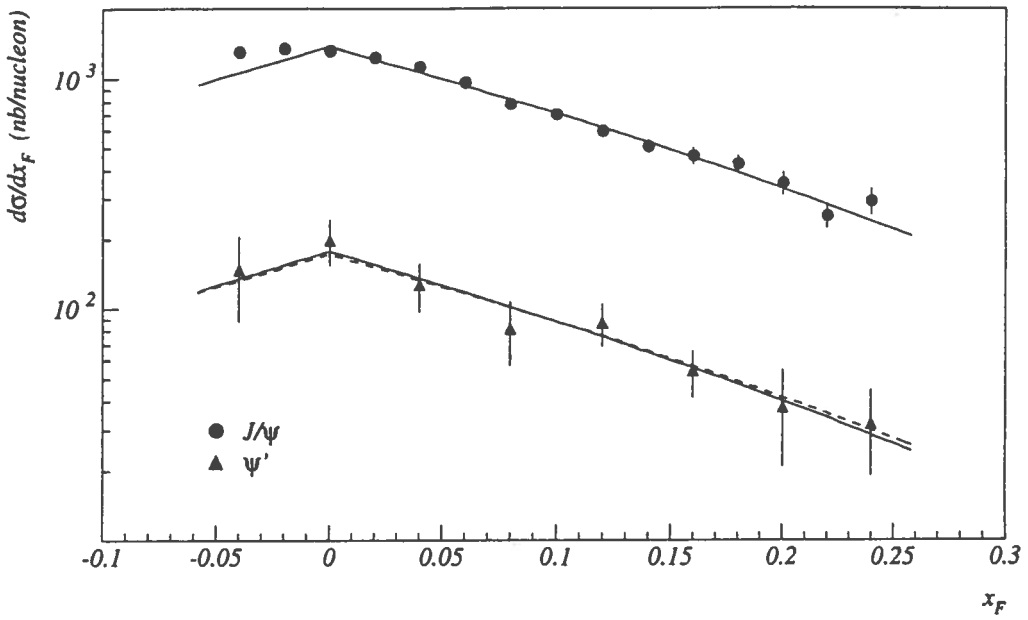

FIG. 4– *Differential cross sections for J/ψ and ψ' versus x_F. The 8 % (J/ψ) and 23 % (ψ') systematic uncertainties due to the normalization are not shown. Superimposed on the data are the fits described in the text. The dashed line is a fit to the ψ' data with the exponential parameter fixed to the corresponding value for J/ψ.*

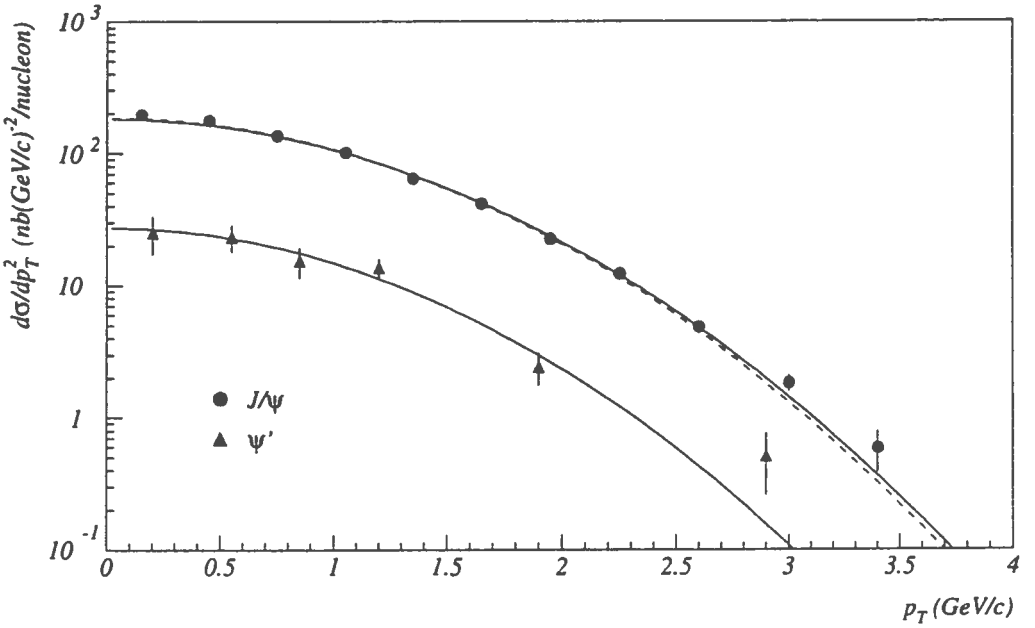

FIG. 5– *Differential cross sections for J/ψ and ψ' versus p_T. The errors shown are just statistical. Superimposed on the data are the fits described in the text. The dashed line is a fit to the J/ψ data performed by excluding the last two points.*

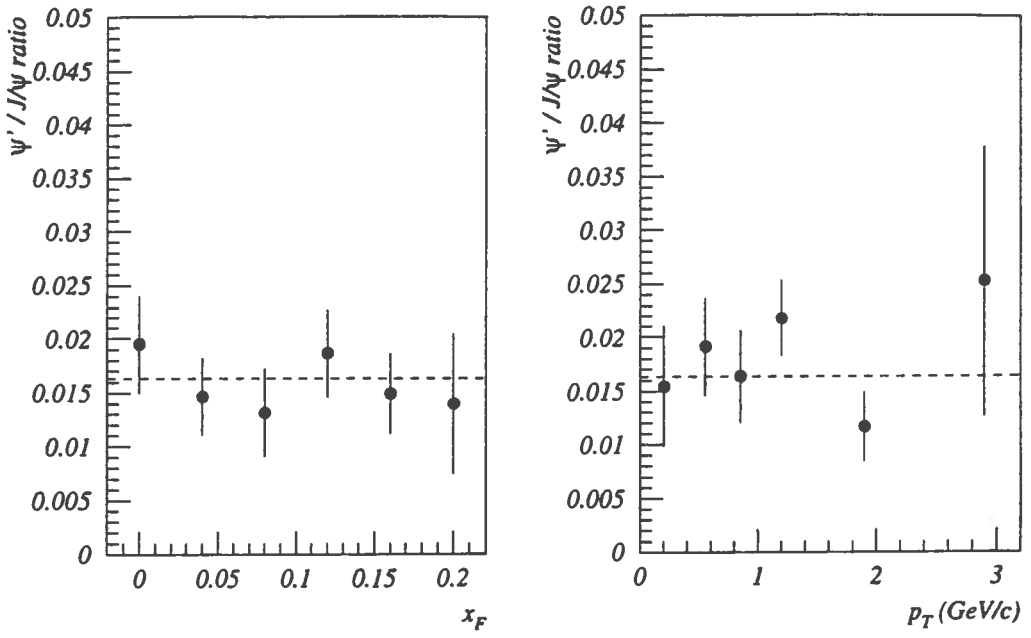

FIG. 6– *Ratio* $B(\psi' \to \mu^+\mu^-) \times \sigma(\psi')$ *to* $B(J/\psi \to \mu^+\mu^-) \times \sigma(J/\psi)$ *versus* x_F *and* p_T.

where a smaller range of p_T is used. The parameters of this fit are listed in the sixth row of Tab. 3.

It is worth noticing that, within experimental errors, both differential cross sections for the two charmonium states are described by the same parameters, suggesting that they are produced by the same mechanisms. In fact, Fig. 6 shows that there is no evident dependence on x_F and p_T of the ratio:

$$\frac{B(\psi' \to \mu^+\mu^-)\sigma(\psi')}{B(J/\psi \to \mu^+\mu^-)\sigma(J/\psi)}, \tag{4}$$

in which the uncertainties in the absolute normalization and the systematics arising from the knowledge of the branching ratios cancel out. These results seem to disagree with recently published data at same energy [13] where a mild increase in this ratio with x_F and p_T is reported.

In Fig. 7 and Fig. 8 we compare our x_F and p_T distributions for the J/ψ and ψ' with those of Fermilab E789 [13].

The cross sections of the two experiments differ by an overall scale factor because of a different choice of the parameter α (E789 uses $\alpha = 0.9$, instead of $\alpha = 0.92$ which gives a difference of about 11 % for the E789 target with $A = 197$).

While the shapes of $d\sigma/dp_T^2$ are in very good agreement, the x_F distributions show some discrepancy ($n_{\mathrm{E789}} = 4.91 \pm 0.18$, $n_{\mathrm{E771}} = 6.38 \pm 0.24$). The nature of this inconsistency is unknown. Nuclear effects due to very different atomic weights of the target [10] would predict an even larger difference in the value of n, though, in this range of x_F, as already pointed out, the value of α can be assumed constant.

In Fig. 7 and Fig. 8 we compare also our results to the theoretical predictions [18] computed using perturbative QCD to leading order for both differential distributions of the two charmonium states. These predictions are still based on the color singlet model [19], because the differential distribution for the most advanced model, developed in the last years, the color octet mechanism [1], are not yet available at low p_T. The contributions of various quarkonium states to the inclusive J/ψ cross section are taken into account by

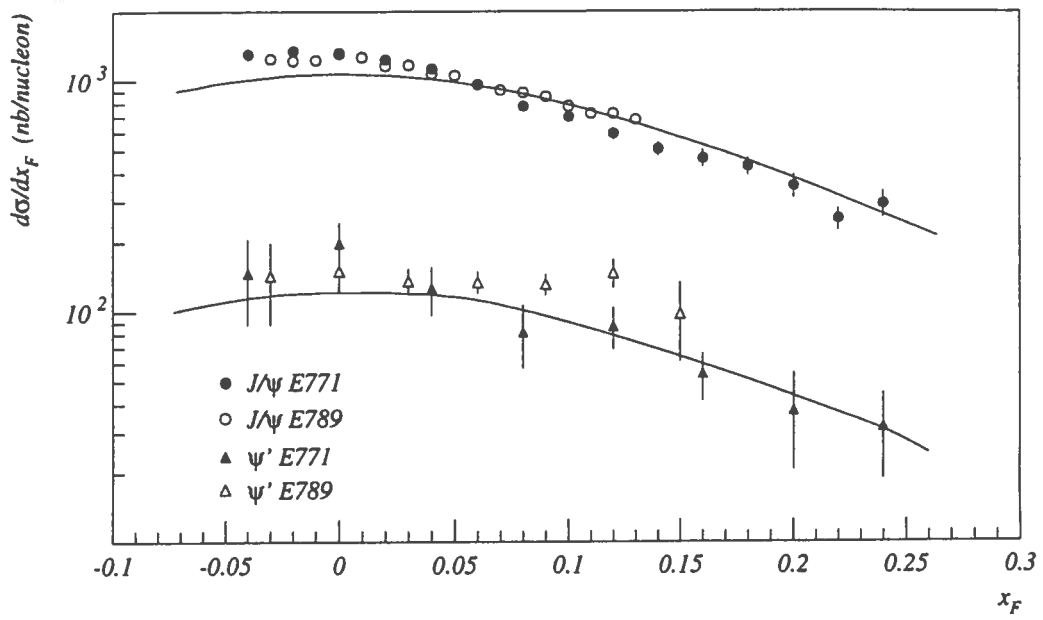

FIG. 7– *E771 differential cross sections versus x_F compared with the E789 data and with the theoretical predictions (full line). Theoretical predictions have been arbitrarily normalized to our data as described in the text.*

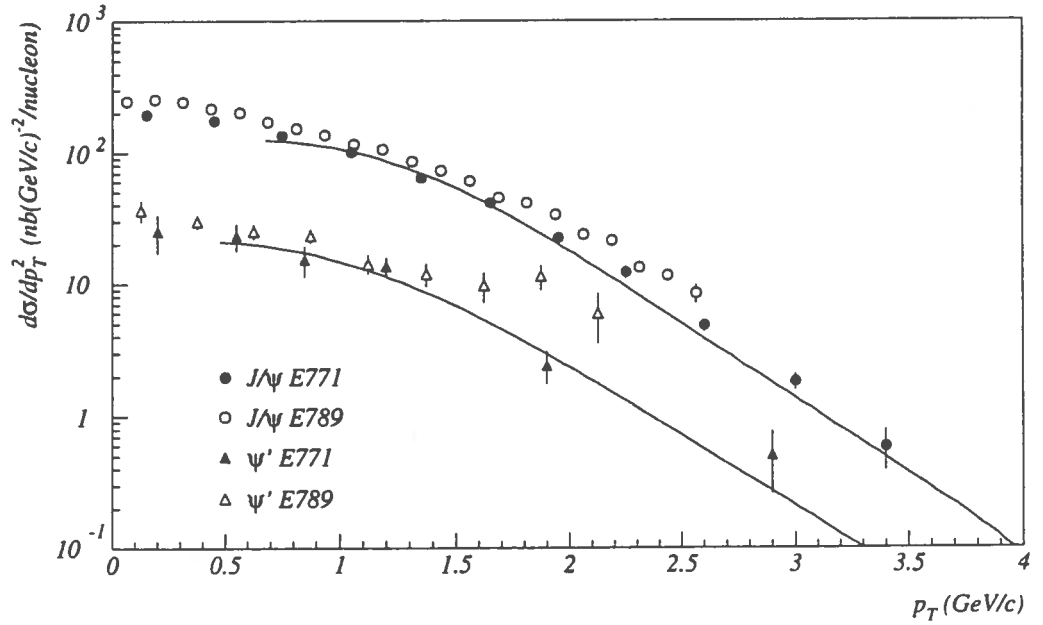

FIG. 8– *E771 differential cross sections versus p_T compared with the E789 data (empty circles) and with the theoretical predictions. Theoretical predictions have been arbitrarily normalized to our data as described in the text.*

using the known branching ratio of the $\chi_{0,1,2}$ and ψ' states decaying in J/ψ [16]. The Martin-Roberts-Stirling set D0 (MRS D0) [15] for the parton structure function has been used for comparison with our data.

Both the shapes and the scale of the theoretical predictions disagree with our data for the $d\sigma/dx_F$ cross sections. The K factors needed to normalize the curves are $K \approx 4$ for J/ψ and $K \approx 16$ for ψ' while the disagreement in shape is mainly at small x_F.

The shape of $d\sigma/dp_T^2$ cross sections is in good agreement with our data, but still needs a scale factor for the normalization. In this case $K \approx 9$ for J/ψ, while for ψ', $K \approx 14$ needs to be used. These $d\sigma/dp_T^2$ predictions are obtained by assuming an intrinsic p_T Gaussian distribution for the partons with $\langle p_T^2 \rangle = 0.5\ (GeV/c)^2$. To eliminate the divergences at low p_T due to χ_{c0} and χ_{c2} states we had to apply an arbitrary cutoff at 0.6 GeV/c for the J/ψ and at 0.4 GeV/c for the ψ'. In fact, the listed K factors depend strongly on the choice of this cut and therefore are experiment dependent.

We also computed the total cross sections for J/ψ and ψ'. Assuming that Eq. (2) describes all the x_F range, we get $\sigma(J/\psi) = (375 \pm 4 \pm 30)\ nb$ and $\sigma(\psi') = (46 \pm 3 \pm 10)\ nb$. These values are consistent with those obtained in Par. 4.1 and with a recent computation of the total cross section using the color octet model [2].

4.3 J/ψ polarization

The same procedure, as in the previous section, was used to obtain the $d\sigma/dcos\theta$ differential cross section shown in Fig. 9. The angle θ is defined as the angle between the positive muon and beam direction in the J/ψ rest frame. In this case the fit has been performed with the function:

$$A(1 + \alpha cos^2\theta)\,, \tag{5}$$

obtaining $\alpha = -0.09 \pm 0.12$. This result is in disagreement with the color octet model [2] which predicts a sizable J/ψ transverse polarization, emphasizing the need for the inclusion of higher twist terms in the description of quarkonium production.

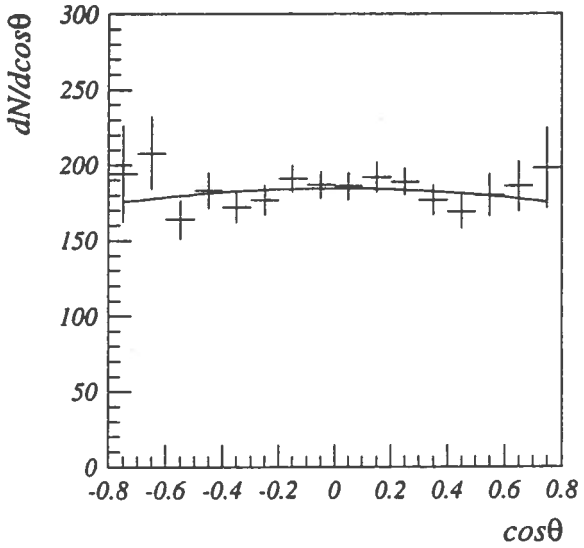

FIG. 9– *cosθ differential cross section. Superimposed on the data is the fit described in the text.*

ACKNOWLEDGMENTS

We thank M.L.Mangano for his support and the discussions about the QCD theoretical distributions. We acknowledge the invaluable help of the Fermilab staff including the Research and Computing Division personnel. This work was supported by the U.S. Department of Energy, the National Science Foundation, the Natural Science and Engineering Research Council of Canada, the Istituto Nazionale di Fisica Nucleare of Italy and the Texas Advanced Research Program.

REFERENCES

[1] E. Braaten and S. Fleming, Phys. Rev. Lett. **74**, 3327 (1995), P. Cho and A.K. Leibovich, Phys. Rev. D **53**, 150 (1996).

[2] M. Beneke and I.Z. Rothstein, SLAC-Pub-7129, March 1996.

[3] CDF Collaboration, F. Abe *et al.*, Fermilab-Conf-94/136, F. Abe *et al.*, Fermilab-Conf-95/128.

[4] T. Alexopoulos *et al.*, Nucl. Phys. B **27**, 257 (1992).

[5] T. Alexopoulos *et al.*, Nucl. Instr. and Meth. A **376**, 375 (1996).

[6] L. Spiegel *et al.*, FERMILAB-TM-1765, (1991).

[7] G. Cataldi *et al.*, Nucl. Instr. and Meth. A **337**, 350 (1994).

[8] L. Antoniazzi *et al.*, Nucl. Instr. and Meth. A **355**, 320 (1995).

[9] L. Antoniazzi *et al.*, Nucl. Instr. and Meth. A **360**, 334 (1995).

[10] M.R. Alde *et al.*, Phys. Rev. Lett. **66**, 133 (1991).

[11] M.J. Leitch *et al.*, Phys. Rev. D **52**, 4251 (1995).

[12] G.A. Schuler, CERN Preprint CERN-TH.7170/94 (1994).

[13] M.H. Schub *et al.*, Phys. Rev. D **52**, 1307 (1995).

[14] V. Abramov *et al.*, FNAL Preprint FERMILAB-PUB-91/62-E (1991), L. Antoniazzi *et al.*, Phys. Rev. D **46**, 4828 (1992) and references therein.

[15] A.D. Martin, W.J. Stirling and R.G. Roberts, Phys. Lett B **306**, 145 (1993).

[16] Particle Data Group, L. Montanet *et. al.*, Phys. Rev. D **50**, 1173 (1994).

[17] W.K. Tang *et al.*, SLAC Preprint SLAC-PUB-6576 (1994), R.Gavai *et al.*, CERN Preprint CERN-TH 7526/94.

[18] M.L. Mangano (private communication), Quarkonium Productions Codes (unpublished).

[19] E.L. Berger and D. Jones, Phys Rev. D **23**, 1521 (1981), B. Guberina *et al.*, Nucl. Phys. B **174**, 317 (1981), R. Bayer and R. Rückl, Z. Phys. C **19**, 251 (1983), B. Humbert, Phys. Lett. B **184**, 105 (1987), R. Gastmans *et al.*, Nucl. Phys. B **291**, 731 (1987).